

Yuanhai Su^{1,2}
Guangwen Chen¹
Quan Yuan¹

Effect of Viscosity on the Hydrodynamics of Liquid Processes in Microchannels

¹ Dalian National Laboratory for Clean Energy, Dalian Institute of Chemical Physics, Chinese Academy of Sciences, Dalian, China.

² Chair of Fluid Process Engineering, Faculty of Mechanical Engineering, University of Paderborn, Paderborn, Germany.

The hydrodynamics of single-phase liquid flow with relatively high fluid viscosities in a microchannel was investigated experimentally. The results showed that the conventional theory could predict the single-phase flow with high fluid viscosities in microchannels. Furthermore, the effect of viscosity on the slug flow of two immiscible liquid phases in a microchannel was studied with high-speed imaging techniques. It was found that a higher dispersed-phase viscosity quickened the flow pattern transition from slug flow to parallel flow and resulted in smaller slugs. A modified capillary number representing the mutual effects of the viscosities of the continuous phase and the dispersed phase was proposed for predicting the slug sizes in microchannels.

Keywords: Hydrodynamics, Microchannel, Microreactor, Multiphase flow, Slug flow, Viscosity

Received: August 04, 2013; *revised:* August 18, 2013; *accepted:* October 11, 2013

DOI: 10.1002/ceat.201300468

1 Introduction

In order to meet the demands of global competition and trade, the current trend in chemical industry is to develop highly efficient, perfectly safe, and environmentally benign methods to produce chemicals. Microreaction technology as one of the most important process intensification technologies has experienced spectacular developments, the advantages of which are obvious for chemical production, such as continuous operational mode, enhanced heat and mass transfer, well-defined flow properties, improved chemistry and excellent process safety, etc. [1–7]. A considerable variety of microscale devices including micromixers, microreactors, micro-heat exchangers, and micro-separators have been designed, in which microchannels are the most important basic units. The characteristics of the hydrodynamics in microchannels are fundamental to understand the principles of transport and reaction processes in microscale devices.

From a practical point of view, the laminar flow in microchannels with diameters of several hundred micrometers where compressible and rarefaction effects are thought to be negligible is of highest interest [8]. The friction factor (f) or the product of the friction factor and the Reynolds number (Re), i.e., the Poiseuille number (Po), is usually used to characterize the hydrodynamics in microchannels. Some previous investigations showed that the experimental value of Po was obviously larger or lower than the values predicted by the conventional theories [9–15]. Nevertheless, more and more in-

vestigations demonstrate that the conventional theories can predict the single-phase flow phenomena in microchannels [16–22]. The fluids used in these previous investigations were mainly water or nitrogen, which have an extremely low viscosity. Furthermore, fluids with high viscosities are usually involved in many chemical processes, e.g., nitration, sulfonation, chemical reactions of polymers, ionic liquid synthesis, etc. However, the hydrodynamics of such kinds of fluids with high viscosities in microchannels has hardly been investigated up to now [23].

In addition, multiphase systems, especially immiscible liquid-liquid two-phase systems, can be used to produce a large variety of intermediate and terminal chemicals. The hydrodynamics and mass transfer characteristics of immiscible liquid-liquid two-phase systems in microchannels are widely investigated due to their importance. Their hydrodynamics in microchannels is much more complicated compared to that of single-phase liquid flow. It depends on different factors, such as the fluid properties, the flow rates of the two phases, and the geometry and surface properties of the microchannel. Zhao et al. [24] studied the flow patterns of two immiscible liquid-liquid phases in T-junction microchannels. Several flow patterns, including droplet, slug, parallel, and annular flows, were identified in microchannels, depending on the competition between the interfacial tension and the inertia force. In particular, the mass transfer rate in slug flow is very high, which shows great potential for applications in different fields, such as the measurement of kinetic parameters of fast reactions [25], protein crystallization [26], nanoparticle synthesis [27], separation processes [28], and the improvement of the selectivity in fast reactions [29]. In slug flow, one liquid flows as a continuous phase while the other liquid (dispersed phase) flows in the form of slugs that are longer than the diameter of the microchannel. The slugs are surrounded with thin liquid films formed by the continuous phase. Slug flow usually occurs

Correspondence: Dr. Guangwen Chen (gwchen@dicp.ac.cn), Dalian National Laboratory for Clean Energy, Dalian Institute of Chemical Physics, Chinese Academy of Sciences, Dalian 116023, China.

at low or moderate flow rates with a volumetric flux ratio of the two phases close to 1. The internal circulation in each slug and the concentration gradient between the slugs and the continuous phase both result in fast mass transfer [30]. Although many researchers have investigated slug flow in microchannels and exploited its relevant applications, only a few studies dealt with the effect of viscosity on this important flow pattern [31, 32]. Therefore, a thorough study on the effect of viscosity on slug flow is necessary.

In this work, the main objective is to study the effect of viscosity on the hydrodynamics of the liquid processes in microchannels. The pressure drop in the microchannel was investigated experimentally for a single-phase liquid flow with different viscosities. The friction factor and the Poiseuille number in the microchannel were compared with those predicted by the conventional laminar flow theory. Moreover, the effects of the fluid viscosity and the wettability of the microchannel walls on the mechanisms of slug flow formation in the microchannels were studied with high-speed imaging techniques. The effects of the flow rates of two immiscible liquid phases on the slug size of the dispersed phase were also studied in detail. A modified capillary number and a correlation are proposed for predicting the slug size in microchannels.

2 Experimental

2.1 Experimental Procedure

Glycerol aqueous solutions were used as the working fluids. The viscosities were measured by a precise digital rotating viscometer (Brookfield-LV; measurement accuracy: ± 0.1 mPa s), and the temperatures of the fluids were controlled by a heating-cooling circulator (Julabo Technology Co., Ltd; F12-ED, measurement accuracy: ± 0.1 °C). Different fluid systems could be obtained by changing the glycerol content in the aqueous solution or by changing the temperature, as shown in Tab. 1. The kerosene-glycerol aqueous solution systems were applied in the two-phase flow experiments. An oil-soluble surfactant, Span 80 (Sorbitan monooleate), was added into kerosene in order to improve the wettability of the microchannel walls and to reduce the interfacial tension between the two immiscible liquid phases. The optical instrument (Dataphysics OCA15) was used to measure the contact angle between the aqueous phase and the poly(methyl methacrylate) (PMMA) plate and the interfacial tension between the two immiscible liquid phases, on the basis of the sessile drop method and the pendant drop method, respectively.

Table 1. Different experimental systems and their viscosities for the single-phase experiments.

	System									
	A	B	C	D	E	F	G	H	I	
T [°C]	25	25	25	25	25	25	30	40	50	
Glycerol content [wt %]	70	75	78	81.3	85	88	85	85	85	
Viscosity [mPa s]	17.67	28.9	39.06	57.59	84.38	134.5	60	33.3	21.3	

Two rectangular microchannels were fabricated in the transparent and smooth PMMA plates by the micromachining technology (FANUCKPC-30a) in our CNC Machining Center. Microchannels 1 and 2 were used for the single-phase flow experiment and the two-phase flow experiment, respectively. For microchannel 1, the depth, width and length were 0.6, 0.6 and 88 mm, respectively. Two orifices with a diameter of 0.6 mm were fabricated for the connection of the pressure measurement tubes. The section for the pressure drop measurement (ΔL) was located in the middle part of microchannel 1, the length of which was 29.7 mm. A polytetrafluoroethylene (PTFE) circular pipeline (internal diameter: 2 mm, length: 3 m) was connected to the inlet of microchannel 1. For microchannel 2, the depth, width and length of the main channel were 0.5, 0.5 and 50 mm, respectively. The depth, width and length of the two inlet channels were 0.5, 0.5 and 15 mm, respectively. The angle between the two inlet channels was 90°.

For the single-phase flow experiment, the glycerol aqueous solution was fed into microchannel 1 through the long PTFE pipeline by a high-precision piston pump (Beijing Satellite Manufacturing Factory; measurement range: 0–10 mL min⁻¹, precision: ± 3 %). Both the pipeline and microchannel 1 were immersed in the water bath of the heating-cooling circulator in order to obtain uniform temperatures. For the two-phase flow experiment, two piston pumps were used (Beijing Satellite Manufacturing Factory; measurement range: 0–5 mL min⁻¹, precision: ± 3 %). The kerosene (continuous phase) was introduced from the longitudinal inlet to the main channel, and the aqueous solution (dispersed phase) was introduced from the lateral inlet. The flow patterns were observed and identified by a high-speed complementary metal oxide semiconductor (CMOS) camera system (Basler; A504kc). Every experimental run was repeated at least three times to ensure reproducibility.

2.2 Conventional Theory for the Hydrodynamics of Single-Phase Flow in Microchannels

In order to correctly understand the experimental results on the hydrodynamics of single-phase flow in microchannels, some factors such as the entrance effect and the measurement error should be considered. The calculated entrance length (L_c) should be shorter than the distance between the inlet and the test section (L_F), in order to ensure fully developed laminar flow in the test section. The calculated entrance length for microchannel 1 is defined by the following equations [33]:

$$L_c = 0.09 \text{Re} D_e \quad (1)$$

$$D_e = \frac{2WH}{W+H} \quad (2)$$

$$\text{Re} = \frac{2\rho Q}{\mu(W+H)} \quad (3)$$

where W and H are the width and the depth of microchannel 1; D_e , ρ , μ , and Q are the hydraulic diameter of microchannel 1 and the density, viscosity and volumetric flow rate of the glycerol aqueous solution, respectively. The Reynolds number in the single-phase flow experiment was less than 100. The calculated entrance length did not exceed 5.4 mm, which was obviously less than the value of L_F (29 mm). Therefore, the flow in the test section was confirmed to be fully developed laminar flow. The pressure gradient (P_{exp}), the friction factor (f_{exp}), and the Poiseuille number (Po_{exp}) can be further calculated according to the measured pressure drop (ΔP) in microchannel 1 [20]:

$$P_{exp} = \frac{\Delta P}{\Delta L} \quad (4)$$

$$f_{exp} = \frac{4\Delta P H^3 W^3}{\rho \Delta L Q^2 (H + W)} \quad (5)$$

$$Po_{exp} = f_{exp} Re = \frac{8\Delta P H^3 W^3}{\Delta L Q \mu (H + W)^2} \quad (6)$$

When the isothermal and incompressible conditions are satisfied and the flow is within the fully developed laminar flow regime, the Poiseuille number in the rectangular channels can be calculated based on the Navier–Stokes equation, which is expressed as follows:

$$\begin{aligned} Po_p &= f Re \\ &= 96(1 - 1.3553a + 1.9467a^2 - 1.7012a^3 \\ &\quad + 0.9564a^4 - 0.2537a^5) \end{aligned} \quad (7)$$

where a is the ratio of the depth to the width of the channel. The depth and width of microchannel 1 used in this section were both 0.6 mm, so the value of a was equal to 1. Therefore, the predicted value of the Poiseuille number (Po_p) on the basis of the conventional laminar flow theory was 56.9.

3 Results and Discussion

3.1 Effects of Flow Rate and Viscosity on the Pressure Drop for Single-Phase Flow

Fig. 1 shows the effects of the flow rate and viscosity on the pressure drop for the single-phase flow in microchannel 1. The glycerol content in the aqueous solution was changed at the same temperature (25 °C, Fig. 1 A) or the glycerol content was kept constant and the temperature was varied (Fig. 1 B). As shown in Fig. 1, the pressure drop in microchannel 1 increased with increasing flow velocity and viscosity, and there was a strictly linear relationship between the pressure drop and the flow velocity for the fluids with different viscosities. From Fig. 1 B, it also can be seen that the temperature can greatly affect the pressure drop in the microchannel by changing the fluid viscosity. To keep the temperature at a steady value is therefore crucial for the accuracy of the experimental results.

Some dimensionless parameters such as the friction factor and the Poiseuille number can be used to describe the flow characteristics in channels. The experimental values of the friction factor (f_{exp}) and the Poiseuille number (Po_{exp}) in microchannel 1 can be calculated by Eqs. (5) and (6). From Fig. 2, it can be seen that the experimental friction factor was inversely proportional to the Reynolds number. The line predicted by the conventional theory ($f = 56.9/Re$) is also plotted in Fig. 2, for com-

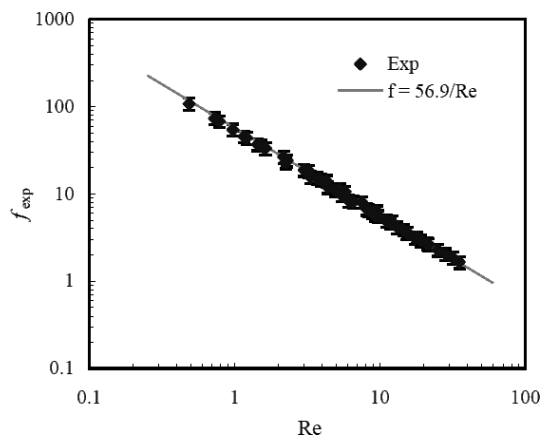


Figure 2. Effect of Re on the friction factor in microchannel 1.

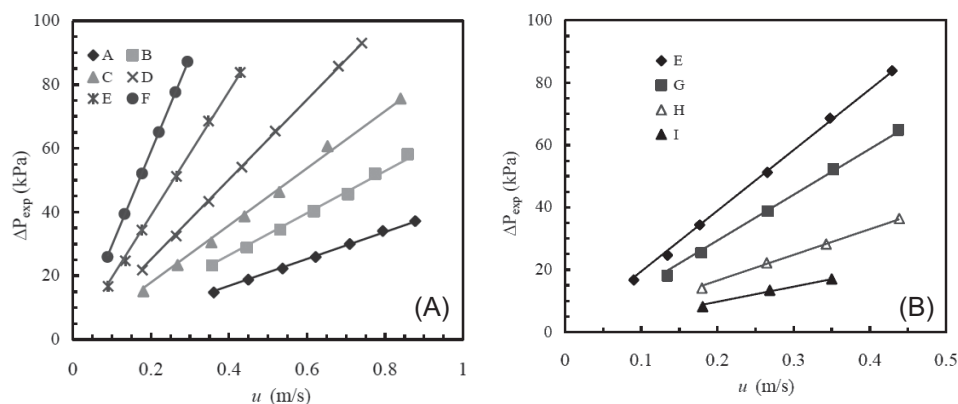


Figure 1. Effects of the flow velocity and viscosity on the pressure drop in microchannel 1. (A) Changing glycerol content in the glycerol aqueous solution, (B) changing temperature of the glycerol aqueous solution.

parison. The experimental friction factor showed close agreement with the value predicted by the conventional theory, with consideration of the measurement uncertainty. In addition, the experimental values of the Poiseuille number were nearly independent of Re and fluctuated weakly around the predicted value from the conventional theory (56.9). These results demonstrated that the single-phase flow with high fluid viscosities in microchannels can be predicted by the conventional theory.

3.2 Effect of Viscosity on the Slug Flow Formation of the Two Immiscible Liquid Phases

In this section, the effect of viscosity on the slug flow formation of the two immiscible liquid phases in microchannel 2 was investigated. Kerosene and water were first used as the working system. However, it was found that only disordered flow patterns were observed, which were not easy to study quantitatively. Therefore, an oil-soluble surfactant, Span 80, was added into kerosene in order to improve the wettability of the microchannel walls and to reduce the interfacial tension between the two immiscible liquid phases. As the content of Span 80 in kerosene was varied from 0 to 1.6 wt %, the contact angle of water in contact with the PMMA wall surface (immersed in the organic phase) was increased from 120° to 149° . The interfacial tension was obviously reduced from 38.2 to 4.12 mN m^{-1} . Under the effect of the surfactant, ordered aqueous phase slugs could be formed easily in microchannel 2. As described above, glycerol was added to water at different contents, so the viscosity of the aqueous solution was changed accordingly. Water and 30, 50, 60 and 70 wt % glycerol aqueous solutions were used as dispersed phases, and their corresponding viscosities were 0.96, 2.3, 5.58, 10.15, and 20.78 mPa s at room temperature ($22 \pm 0.5^\circ \text{C}$), respectively. The interfacial tension between the continuous and dispersed phases was kept almost constant (4.12 mN m^{-1}) when the content of glycerol in the dispersed phase was changed. The contact angle of the dispersed phase in contact with the PMMA wall surface (immersed in the continuous phase) was reduced from 149° to 131° as the glycerol content was increased from 0 to 30 wt %, and then its value was maintained at 131° while increasing the glycerol content.

The formation of slug flow in microchannels is caused by the mutual competition between different forces, such as interfacial tension, viscous force, and inertia force. Several mechanisms such as squeezing, dripping and transition regimes have been proposed [24, 34–36]. Fig. 3 shows the formation processes of slugs in the T-shaped junction of microchannel 2 for two different dispersed-phase viscosities (2.3 and 10.2 mPa s), where the superficial velocities of the continuous and dispersed phases (u_c and u_d) were 0.04 and 0.0133 m s^{-1} , respectively. From Fig. 3, it can be seen that the slug formation processes for these two different dispersed-phase viscosities were similar to each other, which could be explained by the squeezing regime. The two immiscible liquid phases formed an interface at the junction zone of microchannel 2, and the tip of the dispersed phase moved forward by expanding its size (Fig. 3 A (a–c) and Fig. 3 B (a–c)). The tip was further elongated and began to block most of the entire cross-section of microchannel 2 when the diameter of the tip was almost equal to the width of microchannel 2 (Fig. 3 A (d) and Fig. 3 B (d)). Then the pressure in the continuous phase increased dramatically due to less available space, which led to the squeezing of the dispersed-phase neck. The dispersed-phase neck gradually collapsed and a

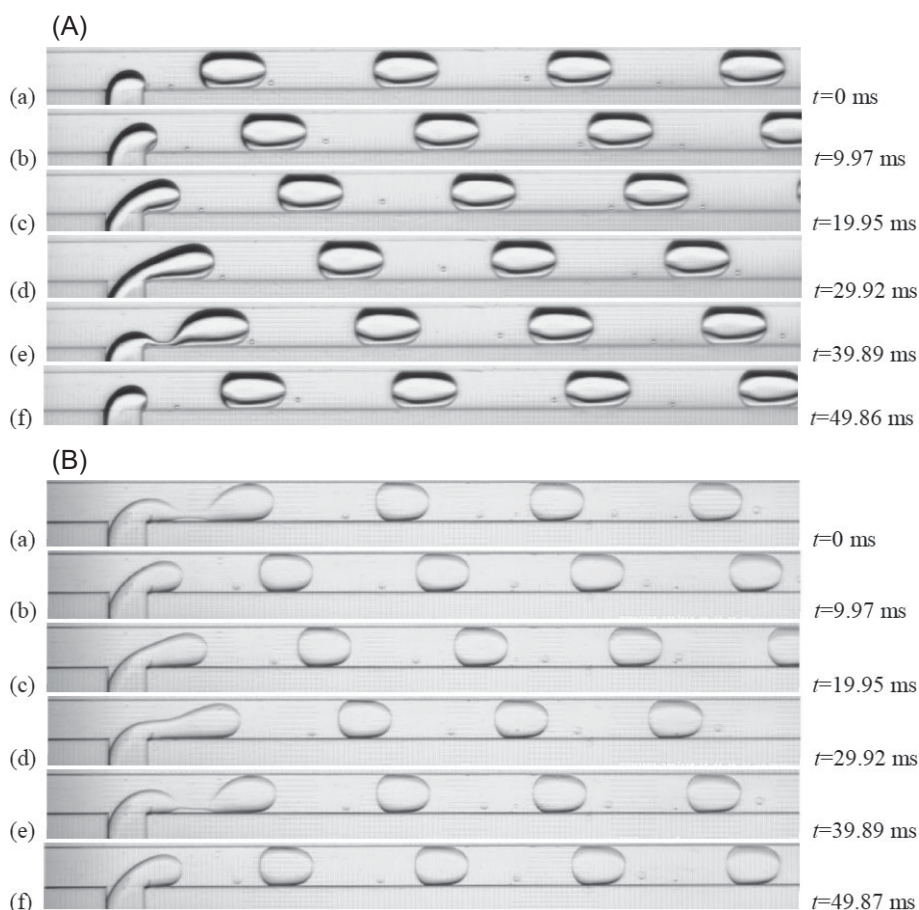


Figure 3. Typical images of the slug formation process in the microchannel ($Q_c = 0.6 \text{ mL min}^{-1}$, $u_c = 0.04 \text{ m s}^{-1}$, $Q_d = 0.2 \text{ mL min}^{-1}$, $u_d = 0.0133 \text{ m s}^{-1}$). (A) Kerosene (1.6 wt % Span 80)–30 wt % glycerol aqueous solution system, (B) kerosene (1.6 wt % Span 80)–60 wt % glycerol aqueous solution system.

thread was formed. Finally, the tiny thread was pinched off and the slug formed (Fig. 3 A (e, f) and Fig. 3 B (e, f)). A new cycle started when the whole formation process was finished. It is obvious that the position for the rupture of the dispersed phase with a lower viscosity was close to the T-junction of microchannel 2, and the dispersed-phase neck contacted with the microchannel wall (Fig. 3 A (e)). However, the position for the rupture of the dispersed phase with a higher viscosity was a little farther from the T-junction, and the thread was surrounded by the continuous phase when it was broken off (Fig. 3 B (e)).

As the dispersed-phase flow rate was further increased ($u_d = 0.02 \text{ m s}^{-1}$), the slug formation process still occurred at the junction of microchannel 2 for the dispersed phase with a low viscosity (Fig. 4 A). For the dispersed phase with a higher viscosity, parallel flow was formed in the front of microchannel 2 (Fig. 4 B (a)), and then it evolved to irregular slug flow in the zone farther from the microchannel inlets (Fig. 4 B (b–f)). This kind of irregular flow can be considered as the transition pattern from slug flow to parallel flow, and it shows large instability and nonlinearity, with a wavy interface between the two immiscible liquid phases, different slug sizes and formation periods [37]. An increase in the dispersed-phase viscosity can quicken the transition from slug flow to parallel flow in the microchannel. This is attributed to the enhancement of the viscous effect between the two immiscible liquid phases.

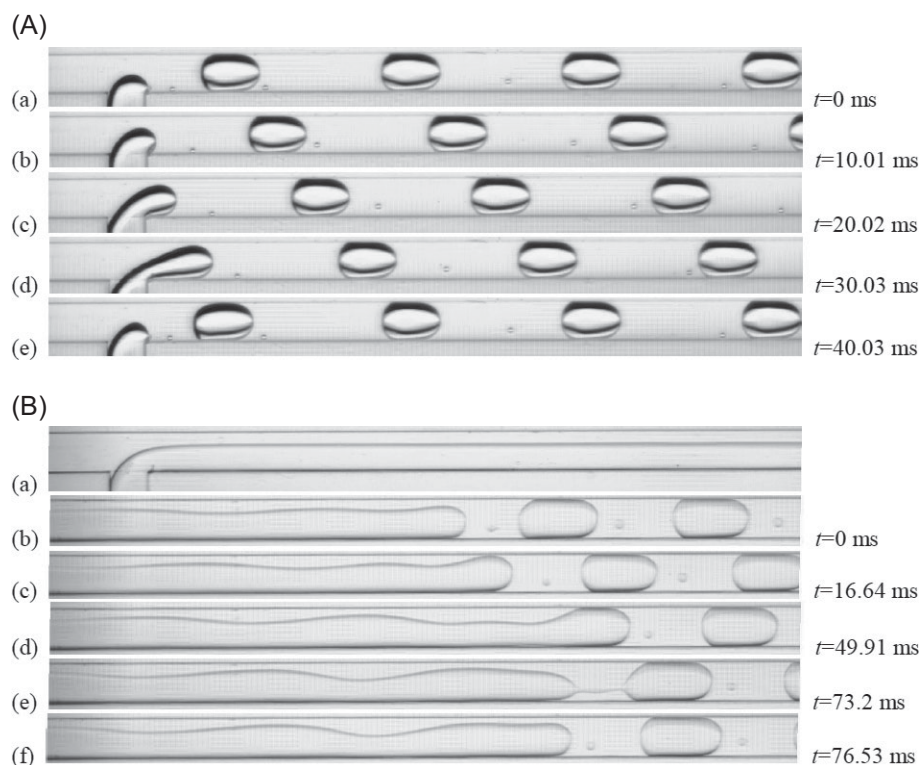


Figure 4. Comparison of slug flow and transition pattern in the microchannel for two systems with different viscosities ($Q_c = 0.6 \text{ mL min}^{-1}$, $u_c = 0.04 \text{ m s}^{-1}$, $Q_d = 0.3 \text{ mL min}^{-1}$, $u_d = 0.02 \text{ m s}^{-1}$). (A) Kerosene (1.6 wt % Span 80)–30 wt % glycerol aqueous solution system, (B) kerosene (1.6 wt % Span 80)–60 wt % glycerol aqueous solution system. (a) Parallel flow in the T-junction. (b–f) The formation process of irregular slugs in the zone was located farther from the microchannel inlets and the distance from the shooting point to the T-junction was about 15 mm.

3.3 Effect of Viscosity on the Slug Size

The rate of mass transfer between the two immiscible liquid phases strongly depends on the contacting condition of the two phases. For a given flow rate of the dispersed phase, generation of a large number of slugs (or droplets) with sizes as small as possible is beneficial to the mass transfer performance, due to the obtained large specific interfacial area. Hence, the factors that determine the slug size in microchannels deserve investigation.

The effect of the dispersed-phase viscosity on the slug length is shown in Fig. 5, where two different continuous-phase superficial velocities were used. From Fig. 5, it can be seen that the slug length decreased with increasing viscosity for most of the immiscible liquid-liquid two-phase systems at the same superficial velocities. However, there was an exceptional condition for the kerosene (1.6 wt % Span 80)–water system, even though it had the same interfacial tension as the other four systems. This is attributed to the higher wettability of the PMMA plate in this system. If the PMMA plate had the same wettability for the kerosene (1.6 wt % Span 80)–water system as those for the other systems, longer slugs in the kerosene (1.6 wt % Span 80)–water system would be obtained due to the lower viscosity of water compared with the glycerol aqueous solutions. Therefore, it can be speculated that the wettability of the microchannel walls for

the two immiscible liquid phases also has an influence on the size of the dispersed-phase slugs. Furthermore, the flow pattern changed from the slug flow to the transition pattern at the dispersed-phase and continuous-phase superficial velocities of 0.02 and 0.04 m s^{-1} when the content of glycerol in the dispersed phase was 50 wt % (Fig. 5 A).

For a higher superficial velocity of the continuous phase (0.0667 m s^{-1}), the steady slug flow did not occur anymore when the dispersed-phase superficial velocity was higher than 0.0267 m s^{-1} (Fig. 5 B). Specially, for the kerosene (1.6 wt % Span 80)–70 wt % glycerol aqueous solution system, slug flow only occurred when the dispersed-phase superficial velocity was lower than 0.00667 m s^{-1} for these two continuous-phase flow rates. The flow pattern easily changed to parallel flow as the dispersed-phase superficial velocity was further increased. These results demonstrate that an increase in the dispersed-phase viscosity obviously quickened the transition from slug flow to parallel flow and thus reduced the operational range of slug flow in the microchannel. For the immiscible liquid-liquid two-phase

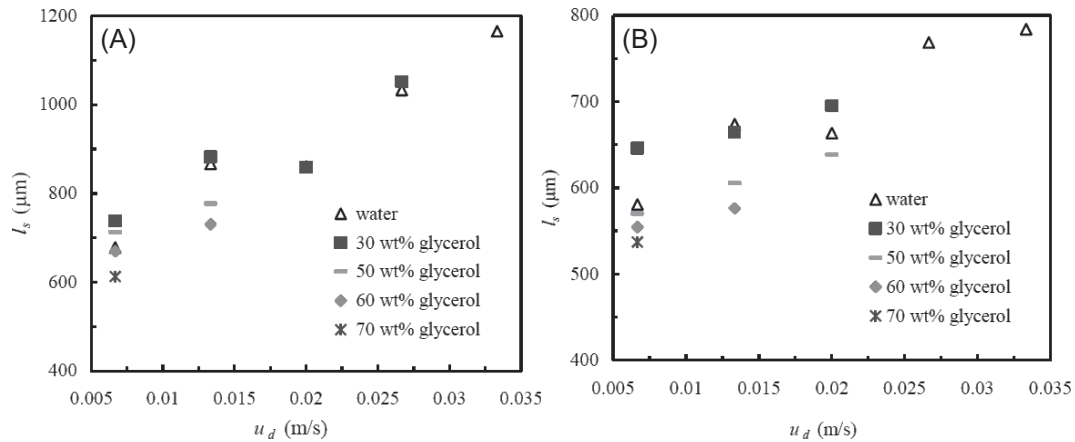


Figure 5. Effect of the dispersed-phase viscosity on the slug size in the microchannel (the lengths of the slugs in the transition pattern are not shown due to their irregularity). (A) $Q_c = 0.6 \text{ mL min}^{-1}$, $u_c = 0.04 \text{ m s}^{-1}$; (B) $Q_c = 1 \text{ mL min}^{-1}$, $u_c = 0.0667 \text{ m s}^{-1}$.

systems with high dispersed-phase viscosities, it is difficult to generate ordered dispersed-phase slugs whose lengths are more than two times the diameter of the microchannel.

3.4 Modified Capillary Number and Correlation for Predicting the Slug Size

Garstecki et al. [36] proposed a correlation for predicting the size of slugs in T-shaped microchannels in the squeezing regime:

$$\frac{l_s}{W} = 1 + \beta \frac{u_d}{u_c} \quad (8)$$

where β can be treated as a fitting parameter and its value depends on the inlet configuration of the microchannel. Even though most of the slug formation processes can be considered in the squeezing regime in this work, it is not possible to correlate the experimental data with this equation. Moreover, the interfacial tension and the viscous force play important roles in the slug formation process. Many researchers used a dimensionless parameter, i.e. the capillary number (Ca), to predict the slug formation process and the slug size in microchannels. The capillary number is defined as the ratio of the viscous force to the interfacial tension:

$$Ca = \mu_c u_c / \sigma \quad (9)$$

where μ_c and u_c are the viscosity and the superficial velocity of the continuous phase, respectively, and σ is the interfacial tension between the two immiscible liquid phases [32, 34, 37]. However, the dispersed-phase viscosity also affects the slug size as discussed above, which is usually not considered by researchers. Here, in order to consider the mutual effects of the viscosities of both the immiscible liquid phases, a modified capillary number is proposed as follows:

$$Ca^* = \mu_m u_c / \sigma = (\varphi_c \mu_c + \varphi_d \mu_d) u_c / \sigma \quad (10)$$

where μ_m is the mean viscosity of the two immiscible liquid phases, μ_d is the dispersed-phase viscosity, and φ_c and φ_d are the volumetric fractions of the continuous phase and the dispersed phase, respectively. In addition, the volumetric flux ratio of the continuous phase to the dispersed phase is also an important factor for the slug size. The following correlation based on multiple linear regression analysis was found to well predict the lengths of the dispersed-phase slugs:

$$\frac{l_s}{D_e} = 0.768 (Ca^*)^{-0.24} \left(\frac{u_d}{u_c}\right)^{0.194} \quad (11)$$

In this correlation, the viscosities of the continuous phase and the dispersed phase are equally emphasized, and their effects on the viscous force during the slug formation process in microchannels are embodied by the modified capillary number. At the same interfacial tension between the two immiscible phases, an increase in the viscous force will be beneficial to the generation of shorter dispersed-phase slugs in the microchannels. However, the interfacial tension tends to inhibit the generation of the dispersed-phase slugs in the microchannels in order to keep the interface energy at a low value. In consequence, the lengths of the dispersed-phase slugs are inversely related to the modified capillary number, which can be explained as a combination effect of the viscous force and the interfacial tension in microchannels. Furthermore, the volumetric flux ratio of the dispersed phase to the continuous phase can be considered as the ratio of the dispersed-phase Weber number to the continuous-phase Weber number in microchannels [24]. An increase in the dispersed-phase superficial velocity leads to a larger dispersed-phase Weber number and thus a larger inertia force in the dispersed phase. The dispersed-phase inertia force tends to maintain the continuity of the disperse-phase flow and to restrain the formation of dispersed-phase slugs in the microchannels. Meanwhile, an increase in the continuous-phase superficial velocity results in a larger continuous-phase Weber number and a higher shear force on the dispersed phase. Hence, the lengths of the dispersed-phase slugs decrease with increasing continuous-phase superficial velocity. Finally, the lengths of the dispersed-phase

slugs are proportional to the volumetric flux ratio of the dispersed phase to the continuous phase, as shown in Eq. (11).

Fig. 6 demonstrates the experimental values of the dimensionless dispersed-phase slug lengths versus the predicted values by Eq. (11). It is worth noting that the data of the kerosene (1.6 wt % Span 80)–water system in Fig. 5 were not used in this correlation. This is because the PMMA plate had a different wettability for this system as compared to the other systems. That is, the effect of the wall wettability on the size of the dispersed phase slugs in the microchannels is not included in Eq. (11). From Fig. 6, it can be seen that the relative deviations between the experimental and predicted values of the dimensionless slug lengths were within $\pm 10\%$. Therefore, the modified capillary number and the correlation are useful for predicting the size of dispersed-phase slugs in microchannels.

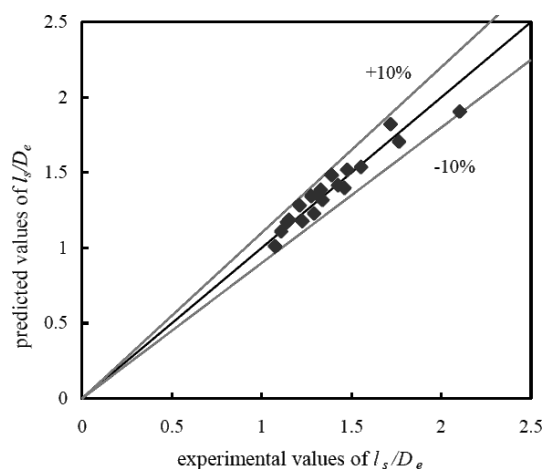


Figure 6. Comparison between the experimental values of the dimensionless slug lengths versus the predicted values.

4 Conclusions

The effect of viscosity on the hydrodynamics of liquid processes in microchannels was investigated experimentally. It was found that the conventional theory could predict the single-phase flow in microchannels with high viscosities. For two-phase flow in microchannels, the dispersed-phase viscosity had an obvious influence on the slug flow formation. A higher dispersed-phase viscosity quickened the transition from slug flow to parallel flow and resulted in smaller dispersed-phase slugs. The ratio of the flow rates of the two immiscible liquid phases also affected the slug size. A modified capillary number that considered the mutual effects of the viscosities of the continuous phase and the dispersed phase was proposed, and a correlation was developed for predicting the slug size in microchannels. This correlation predicts the slug size well, with a relative deviation of $\pm 10\%$.

Acknowledgment

The work reported in this article was financially supported by research grants from the National Natural Science Foundation of China (Nos. 21225627, 21106141), and the Ministry of Science and Technology of China (No. 2012BAA08B02).

The authors have declared no conflict of interest.

Symbols used

Ca	[-]	capillary number
Ca	[-]	modified capillary number
D_e	[m]	hydraulic diameter of the microchannel
f	[-]	friction factor
f_{exp}	[-]	experimental friction factor
H	[m]	microchannel height
ΔL	[m]	measured segment for pressure drop
L_e	[m]	entrance length of the microchannel
L_F	[m]	distance between the microchannel inlet and the test section
l	[μm]	slug length
ΔP	[Pa]	pressure drop
P_{exp}	[N m^{-3}]	experimental pressure gradient
Po	[-]	Poiseuille number
Po_{exp}	[-]	experimental Poiseuille number
Po_p	[-]	predicted Poiseuille number
Q	[mL min^{-1}]	volumetric flow
Q_c	[mL min^{-1}]	continuous-phase volumetric flow
Q_d	[mL min^{-1}]	dispersed-phase volumetric flow
Re	[-]	Reynolds number
u	[m s^{-1}]	flow velocity
u_c	[m s^{-1}]	continuous-phase superficial velocity
u_d	[m s^{-1}]	dispersed-phase superficial velocity
W	[m]	microchannel width

Greek symbols

a	[-]	ratio of the depth to the width of the channel
φ_c	[-]	continuous-phase volumetric fraction
φ_d	[-]	dispersed-phase volumetric fraction
μ	[mPa s]	viscosity
μ_c	[mPa s]	continuous-phase viscosity
μ_d	[mPa s]	dispersed-phase viscosity
μ_m	[mPa s]	mean viscosity of two immiscible liquid phases
ρ	[kg m^{-3}]	mass density
σ	[mN m^{-1}]	interfacial tension between two immiscible liquid phases

Subscripts

c	continuous phase
d	dispersed phase

References

- [1] S. Marre, K. F. Jensen, *Chem. Soc. Rev.* **2010**, 39 (3), 1183.
- [2] T. Noël, S. L. Buchwald, *Chem. Soc. Rev.* **2011**, 40 (10), 5010.
- [3] M. N. Kashid, A. Renken, L. Kiwi-Minsker, *Chem. Eng. Sci.* **2011**, 66 (17), 3876.
- [4] M. Shang, T. Noël, Q. Wang, V. Hessel, *Chem. Eng. Technol.* **2013**, 36 (6), 1001.
- [5] N. Assmann, A. Ladosz, P. Rudolf von Rohr, *Chem. Eng. Technol.* **2013**, 36 (6), 921.
- [6] V. Hessel, D. Kralisch, N. Kochmann, T. Noël, Q. Wang, *ChemSusChem* **2013**, 6 (5), 746.
- [7] A. D. Anastasiou, A. A. Mouza, C. Makatsoris, A. Gavriilidis, *Exp. Therm. Fluid Sci.* **2013**, 44, 90.
- [8] B. Cao, G. W. Chen, Q. Yuan, *Int. Commun. Heat Mass Transf.* **2005**, 32 (9), 1211.
- [9] P. Y. Wu, W. A. Little, *Cryogenics* **1983**, 23 (5), 273.
- [10] G. M. Mala, D. Q. Li, *Int. J. Heat Fluid Flow* **1999**, 20 (2), 142.
- [11] D. Pfund, D. Rector, A. Shekarriz, A. Popescu, J. Welty, *AIChE J.* **2000**, 46 (8), 1496.
- [12] W. L. Qu, G. M. Mala, D. Q. Li, *Int. J. Heat Mass Transf.* **2000**, 43 (21), 353.
- [13] S. B. Choi, R. F. Barron, R. O. Warrington, *ASME Proc.* **1991**, 123.
- [14] D. Yu, R. Warrington, R. Barron, T. Ameel, *Proc. ASME-JSME Therm. Eng. Joint Conf.* **1995**, 523.
- [15] X. N. Jiang, Z. Y. Zhou, X. Y. Huang, C. Y. Liu, *Proc. IEEE/CPMT Electron. Packaging Technol. Conf.* **1997**, 119.
- [16] S. M. Flockhart, R. S. Dhariwal, *J. Fluids Eng.* **1998**, 120 (2), 291.
- [17] B. Xu, K. T. Ooi, N. T. Wong, W. K. Choi, *Int. Commun. Heat Mass Transf.* **2000**, 27 (8), 1165.
- [18] J. Judy, D. Maynes, B. W. Webb, *Int. J. Heat Mass Transf.* **2002**, 45 (17), 3477.
- [19] D. Liu, S. V. Garimella, *Proc. Eighth AIAA/ASME Joint Thermophys. Heat Transf. Conf.* **2002**, 65.
- [20] J. Yue, G. W. Chen, Q. Yuan, *Chem. Eng. J.* **2004**, 102 (1), 11.
- [21] P. Hrnjak, X. Tu, *Int. J. Heat Fluid Flow* **2007**, 28 (1), 2.
- [22] H. J. Su, H. N. Niu, L. W. Pan, S. D. Wang, A. J. Wang, Y. K. Hu, *Ind. Eng. Chem. Res.* **2010**, 49 (8), 3830.
- [23] B. Cortese, T. Noël, M. H. J. M. de Croon, S. Schulze, E. Klemm, V. Hessel, *Macromol. React. Eng.* **2012**, 6 (12), 507.
- [24] Y. C. Zhao, G. W. Chen, Q. Yuan, *AIChE J.* **2006**, 52 (12), 4052.
- [25] H. Song, R. F. Ismagilov, *J. Am. Chem. Soc.* **2003**, 125 (47), 14613.
- [26] B. Zheng, J. D. Tice, L. S. Roach, R. F. Ismagilov, *Angew. Chem., Int. Ed. Engl.* **2004**, 43 (19), 2508.
- [27] S. A. Khan, K. F. Jensen, *Adv. Mater.* **2007**, 19 (18), 2556.
- [28] Y. H. Su, G. W. Chen, Y. C. Zhao, Q. Yuan, *AIChE J.* **2009**, 55 (8), 1948.
- [29] B. Ahmed, D. Barrow, T. Wirth, *Adv. Synth. Catal.* **2006**, 348 (9), 1043.
- [30] J. R. Burns, C. Ramshaw, *Lab Chip* **2001**, 1, 10.
- [31] J. D. Tice, A. D. Lyon, R. F. Ismagilov, *Anal. Chim. Acta* **2004**, 507 (1), 73.
- [32] J. Tan, J. H. Xu, S. W. Li, G. S. Luo, *Chem. Eng. J.* **2008**, 136 (2/3), 306.
- [33] R. K. Shah, A. L. London, *Laminar Flow Forced Convection in Ducts*, Academic Press, New York **1978**.
- [34] J. H. Xu, G. S. Luo, S. W. Li, G. G. Chen, *Lab Chip* **2006**, 6 (1), 131.
- [35] J. Husny, J. J. Cooper-White, *J. Non-Newtonian Fluid. Mech.* **2006**, 137 (1–3), 121.
- [36] P. Garstecki, M. J. Fuerstman, H. A. Stone, G. M. Whitesides, *Lab Chip* **2006**, 6 (3), 437.
- [37] P. Guillot, A. Colin, *Phys. Rev. E* **2005**, 72 (6), 066301.